 ©2000 Kvantovaya Elektronika and Turpion Ltd

*CONTROL OF LASER RADIATION PARAMETERS*

PACS numbers: 42.55.Ah; 42.55.Xi; 42.65.Sf

# Emission spectrum of a solid-state laser with an nonuniform pump distribution along a Fabry – Perot cavity

E A Ovchinnikov, P A Khandokhin, E Yu Shirokov

DOI: 10.1070/QE2000v030n01ABEH001651

**Abstract. The influence of an nonuniform distribution of the unsaturated gain along a cavity on a competitive interaction of longitudinal modes was investigated experimentally and theoretically. This nonuniformity is the result of a partial filling of the cavity by the active medium and of an exponential absorption of the pump radiation along the active element. An analysis is made of the evidence in support of this approach to the description of multimode operation of solid-state lasers with longitudinal inhomogeneous pumping.**

## 1. Introduction

The problem of the influence of a spatially nonuniform distribution of the gain in a solid-state laser on its dynamic characteristics (optical spectrum, polarisation of radiation, etc.) has a long history. This applies particularly to the relationship between the gain nonuniformity along the cavity and the characteristic features of the optical emission spectrum of a laser [1, 2]. It has been observed that the placing of the active medium near the cavity mirrors increases the competition between longitudinal modes, as a result of which a 'rarefaction' of the optical spectrum is observed, i.e. modes separated from one another by more than two mode spacings are involved in the lasing. An increase in mode competition has a simple qualitative explanation. The spatial structure of the normal cavity modes overlap most strongly in the vicinity of the cavity mirrors, because the nodes of all the modes converge on the mirrors. The quantitative manifestation of this effect depends on the specific form of the longitudinal gain nonuniformity.

The appearance of lasers diode-pumped through one of the end-faces of the active element, on which the input mirror of the cavity is as a rule located, has renewed the interest in the characteristic features of the dynamic behaviour resulting from an nonuniform gain distribution within the laser cavity. One of the causes of the longitudinal gain inhomogeneity is a partial filling of the cavity by the active medium. Another cause is the exponential absorption of the pump beam intensity in the course of its propagation along the axis of the active element.

**E A Ovchinnikov, P A Khandokhin, E Yu Shirokov** Institute of Applied Physics, Russian Academy of Sciences, ul. Ul'yanova 46, 603600 Nizhny Novgorod, Russia

Received 19 August 1999
*Kvantovaya Elektronika* **30** (1) 23 – 29 (2000)
Translated by A K Grzybowski

The influence of each type of the gain nonuniformity has been investigated [3, 4]. It was demonstrated experimentally and theoretically in Ref. [3] that a partial filling of the cavity with the active medium can suppress the optical modes with a potentially greater gain (for example, the central mode) by weaker modes. Similar conclusions were reached by other investigators [4], who took into account the exponential decrease in the population inversion from one end-face of the crystal (throughout which pumping takes place) to the other. This communication describes an experimental and theoretical study of the joint effect of the above factors, associated with the longitudinal nonuniformity of the unsaturated gain along the cavity, on the competitive interaction of the longitudinal modes.

## 2. Model of a diode-pumped solid-state laser

The principal features of the behaviour of multimode solid-state lasers are described satisfactorily by the rate equations of Tang, Statz, and deMars [5], which have been thoroughly investigated in the case of a homogeneous distribution of the gain along the cavity [6 – 9];

$$\frac{\mathrm{d}I_k(\tau)}{\mathrm{d}\tau} = GI_k(\tau)\left[g_k\int_0^L n(z,\,\tau)\psi_k^2(z)\,\mathrm{d}z - 1 - \beta_k\right], \qquad (1)$$

$$\frac{\partial n(z,\,\tau)}{\partial\tau} = A(z) - n(z,\,\tau)\left[1 + \sum g_j\,\psi_j^2(z)I_j(\tau)\right]. \qquad (2)$$

Here, $I_k(\tau)$ is the intensity of an individual mode, relative to the saturation field; $n(z,\,\tau)$ is the population inversion density; $\tau = t/T_1$ is time measured in units of the inversion decay time; $z$ is the longitudinal coordinate; $L$ is the optical length of the cavity; $A(z)$ is the pump parameter represented by the unsaturated inversion distribution along the cavity; $\psi_k(z) = \sqrt{2}\sin(\pi q_k z/L)$ is the cavity eigenfunction for the longitudinal modes of a Fabry – Perot cavity; $\pi q_k/L$ is the wave number ($q_k$ is a large integer, equal to the number of $k$th-mode half-waves along the cavity length); $k = 1, 2, \ldots, K$; $K$ is the total number of laser modes under consideration; $G = T_1/T_c$; $T_c$ is the photon lifetime in the cavity; $g_k$ is the gain of the case $k$th mode; $\beta_k$ represents the additional losses in the $k$th mode compared with the standard losses specified by $1/T_c$.

In the simplest case when the pumping is homogeneous along the entire length of the cavity [$A(z) = A_0$], we can go over from integrodifferential equations to a system of ordinary differential equations by expanding the population inversion as an infinite series:

$$n(z,\,\tau) = D_0(\tau) - 2\sum_{k=1}^{K} n_k(\tau)\cos(2\pi q_k z/L) + \ldots, \qquad (3)$$

in which only the expansion terms written out in formula (3) are taken into account; the expansion coefficients appear directly in the equations for the mode intensities. The order of the system is then $2K+1$. The coefficients in the above expansion represent the population inversion averaged over the cavity length and the amplitudes of the spatial inversion gratings with an nonuniformity scale of the order of $\lambda/2$, resulting from inversion 'hole burning' by each optical mode. We emphasise that both the large-scale population-inversion gratings with an nonuniformity scale $\sim L/2(q_i - q_j)$ and the small-scale gratings with an nonuniformity scale $\sim\lambda/4$ have been disregarded in the published rate equations [6–9]. Numerous studies have shown that this approximation is fully justified in description of the low-frequency dynamics of multimode solid-state lasers in the case of a homogeneous distribution of pumping along the cavity.

In a real experiment, the unsaturated gain of the active medium is distributed along the cavity in a manner which is by no means homogeneous. Two alternative approaches to the problem of taking into account the nonuniform gain (population inversion) distribution along the laser cavity axis have been adopted. They differ in the type of expansion of the population inversion of the active medium as a series in terms of the functions $\cos(2\pi Q_i z/L)$ [2–4, 10]. Here the terms $Q_i$ denote both small integers (0, 1, 2, ..., $K-1$) and large integers, which are identical with $q_k$.

A multimode solid-state laser model was rigorously justified by Khandokhin et al. [11]. In order to take into account the spatial nonuniformity of the unsaturated gain of the active medium, the model takes into consideration the individual time-dependent cofactor $\Phi(z)$ [$A(z) = A_0\Phi(z)$] in the expression for the population inversion. The factor describes the unsaturated gain profile:

$$n(z,\tau) = \Phi(z)N(z,\tau)\ . \tag{4}$$

Here, $\Phi(z)$ is determined solely by the geometry of the problem (the crystal size, the exponential variation of the gain along the crystal, etc.) and describes the slow changes in the population inversion along the cavity axis. The new variable $N(z,\tau)$ describes saturation of the inversion population by the generated field [in the absence of the field, we have $N(z,\tau) = A_0$]. This representation of the population inversion leads to the appearance, in the field-intensity equations, of additional terms (compared with the simplest case) describing variation of the competitive mode interaction; the order of the system then remains the same as before ($2K+1$):

$$\begin{aligned}
\frac{\mathrm{d}I_k}{\mathrm{d}\tau} &= GI_k\left[g_k\left(D_0 + \sum_{m=1}^{K} N_m\Phi_{|k-m|}\right) - 1 - \beta_k\right]\ ,\\
\frac{\mathrm{d}D_0}{\mathrm{d}\tau} &= A_0 - D_0\left(1 + \sum_{m=1}^{K} g_m I_m\right) - \sum_{m=1}^{K} g_m I_m N_m\ ,\\
\frac{\mathrm{d}N_k}{\mathrm{d}\tau} &= -\left(1 + \sum_{m=1}^{K} g_m I_m\right)N_k - \frac{1}{2}g_k I_k D_0\ .
\end{aligned} \tag{5}$$

Here, the expansion coefficients $\Phi_j$ are introduced as follows:

$$\Phi_0 = \frac{1}{L}\int_0^L \Phi(z)\,\mathrm{d}z \equiv 1\,, \qquad \Phi_j = \frac{1}{L}\int_0^L \Phi(z)\cos\frac{2\pi jz}{L}\,\mathrm{d}z\ . \tag{6}$$

It must be emphasised once again that the proposed approach takes into account the large-scale population-inversion gratings arising from the longitudinal pumping nonuniformity:

$$D_p^0(\tau) = D_0(\tau)\Phi_p\ .$$

The superscript in $D_p^0(\tau)$ means that these gratings describe the unsaturated large-scale population-inversion profile. In other words, the generated modes do not participate in the formation of these gratings, which is the reason for the absence of the amplitudes $D_p^0(\tau)$ among the variables in the system of equations (5). The total amplitude of a large-scale grating can be represented in the following form:

$$D_p(\tau) \equiv \frac{1}{L}\int_0^L n(z,\tau)\cos\frac{2\pi pz}{L}\,\mathrm{d}z = D_p^0(\tau) + D_p^{\mathrm{s}}(\tau)\ . \tag{7}$$

Here, the term $D_p^{\mathrm{s}}(\tau)$ describes saturation. Allowance for this term by Pieroux and Mandel [10] increased the dimensionality of the system of equations to $3K$. In the proposed model, we neglected the gratings $D_p^{\mathrm{s}}(\tau)$ thus remaining within the framework of the generally adopted approximation with a homogeneous distribution of the unsaturated gain.

In order to compare the experimental data with the theoretical results obtained on the basis of a model described by the system of equations (5), we specified a particular form of the longitudinal and saturated-gain nonuniformity caused by the exponential attenuation of pumping along the crystal, and incomplete filling of the laser cavity, which corresponds to the real experimental conditions:

$$\Phi(z) = \begin{cases} \alpha L\exp(-\alpha z)/[1-\exp(-\alpha l)]\,, & 0 \leqslant z \leqslant l\,,\\ 0\,, & l < z \leqslant L\,. \end{cases} \tag{8}$$

The equality $\Phi_0 = 1$ holds as a result of selection of this type of the distribution function. The remaining expansion coefficients have the form:

$$\begin{aligned}
\Phi_p = \frac{1}{1+q^2p^2}\Bigg[&\frac{\exp(\alpha l) - \cos(2\pi pl/L)}{\exp(\alpha l) - 1}\\
&+ \frac{q^2p^2\alpha l}{\exp(\alpha l) - 1}\,\frac{\sin(2\pi pl/L)}{2\pi pl/L}\Bigg]\ ,
\end{aligned} \tag{9}$$

where $p = 1, 2, \ldots, K-1$; $q = 2\pi/\alpha\varphi$. Expression (9) is converted into the corresponding expressions from Ref. [4] (for $l \to L$) or Refs [2, 3] (for $\alpha \to 0$).

The results of our numerical experiments are presented below together with the experimental data.

## 3. Experimental results

The experimental setup is shown in Fig. 1. Pumping was provided by a diode laser (*1*) generating linearly polarised radiation with $\lambda = 810$ nm. The active element consisted of an Nd:YAG crystal rod (6 mm in diameter, 10 mm long) with its end-faces skewed at an angle of $\sim 1.5^\circ$ relative to one another. The input end-face (*4*), perpendicular to the rod axis and carrying a multilayer dielectric coating, ensured a high reflection coefficient ($\sim 0.995$) at $\lambda = 1064$ nm and a comparatively high transmission coefficient at $\lambda = 810$ nm. The second end-face was antireflection-coated for $\lambda = 1064$ nm. A spherical output mirror (*6*) with a radius of curvature of 30 cm had the reflection coefficient of $\sim 0.99$ at $\lambda = 1064$ nm. Experimental studies were performed for two optical lengths of the cavity (5.7 and 8.4 cm), which corresponded to factors representing filling of the cavity by the active medium (cavity fill factors) of 0.32 and 0.22. A half-wave plate (*8*) and a Glan prism (*10*) were used to investigate the polarisation of the optical spectrum. The spectrum was analysed by a Fabry–Perot etalon [15] with 2.4 and 4.1 mm bases, which

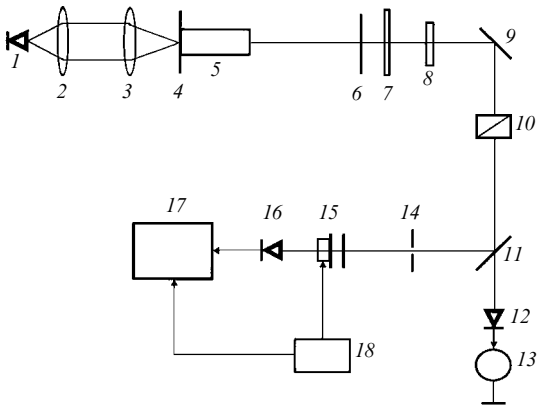


**Figure 1.** Experimental setup: (*1*) pump laser ($\lambda = 810$ nm); (*2*, *3*) collimating lenses; (*4*, *6*) cavity mirrors; (*5*) $Nd^{3+}$:YAG crystal; (*7*) filter ($\lambda = 810$ nm); (*8*) half-wave plate ($\lambda = 1064$ nm); (*9*, *11*) rotation mirrors; (*10*) Glan prism; (*12*, *16*) photodiodes; (*13*) microammeter; (*14*) aperture; (*15*) Fabry–Perot etalon; (*17*) oscilloscope; (*18*) control unit for the Fabry–Perot interferometer.

corresponded to a free spectral range of $\sim$63 and 37 GHz. The finesse $F$ of the etalon was 119.

The quasi-isotropic cavity of an Nd:YAG laser can ensure simultaneous emission of two normal orthogonally polarised systems of the longitudinal cavity modes. The linearly polarised laser-pump radiation introduces a discrimination into the conditions for the excitation of orthogonally polarised modes [12]. With the aid of a $\lambda = 810$ nm half-wave plate (not shown in Fig. 1), the direction of the pump radiation polarisation was chosen to ensure the maximum discrimination of modes with different polarisations. For this reason, systems of 'strong' and 'weak' polarisation modes were observed in the laser radiation. They can be selected for study with the aid of a half-wave plate (*8*) and a polariser (*10*).

Fig. 2 shows typical optical spectra of the strong-polarisation modes of an Nd:YAG laser for $L_{opt} = 8.3$ cm ($\Delta\nu = c/2L_{opt} = 1.8$ GHz). Evidently, the spectral components are

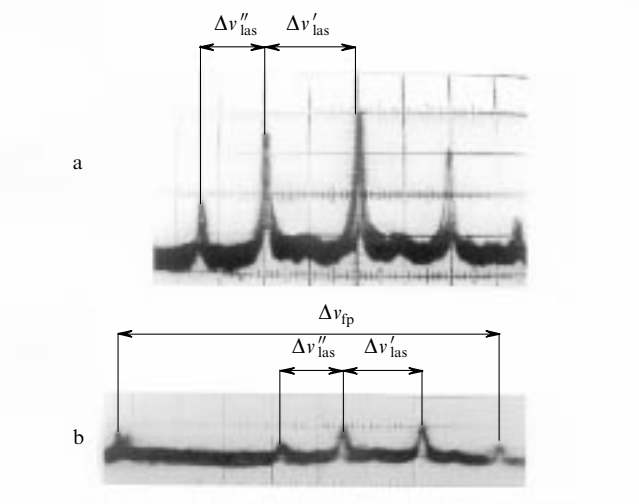


**Figure 2.** Emission spectra of a laser under conditions of dominant polarisation with $L_{opt} = 8.3$ cm, $A = 1.22$ (a), and 1.16 (b); $\Delta\nu'_{las}$, $\Delta\nu''_{las}$ are the frequency intervals between lasing modes; $\Delta\nu_{fp}$ is the mode spacing of the Fabry–Perot etalon.

not equidistant. The spacing $\Delta\nu'_{las}$ between the central mode and the side modes nearest to it is greater than the spacing $\Delta\nu''_{las}$ between pairs of the side modes. The frequency intervals between the generated modes were estimated by comparing them with the mode spacing of the Fabry–Perot etalon $\Delta\nu_{fp} = 37$ GHz (Fig. 2b). When account was taken of the experimental error, the spacings between the generated modes were $\Delta\nu''_{las} = 5.6 \pm 0.7$ and $7.4 \pm 0.9$ GHz. This corresponded approximately to three ($1.3 \times 3 = 5.4$ GHz) and four ($1.8 \times 4 = 7.2$ GHz) mode spacings $\Delta\nu$. Consequently, two or three longitudinal modes were suppressed between the lasing modes.

Fig. 3 presents the dependences of the optical-mode intensities on the pump parameter in both two-dimensional (Fig. 3a) and three-dimensional (Fig. 3b) forms for schematic representations of the positions of the lasing modes on the frequency axis and taking into account the frequency difference between them (in units of the elementary mode spacings $\Delta\nu$).

Fig. 3 demonstrates that, for pump intensities close to the threshold, there was only one lasing mode (mode 8). On increase in the pump intensity, initially the side modes 12 and 4, separated by four mode spacings from the central mode 8, and then the side modes 1 and 15, separated from the neighbouring modes 4 and 12 by three mode spacings, began to lase almost simultaneously. A virtually monotonic increase in the intensities of all the modes involved in lasing was also observed. Jumps between the modes with

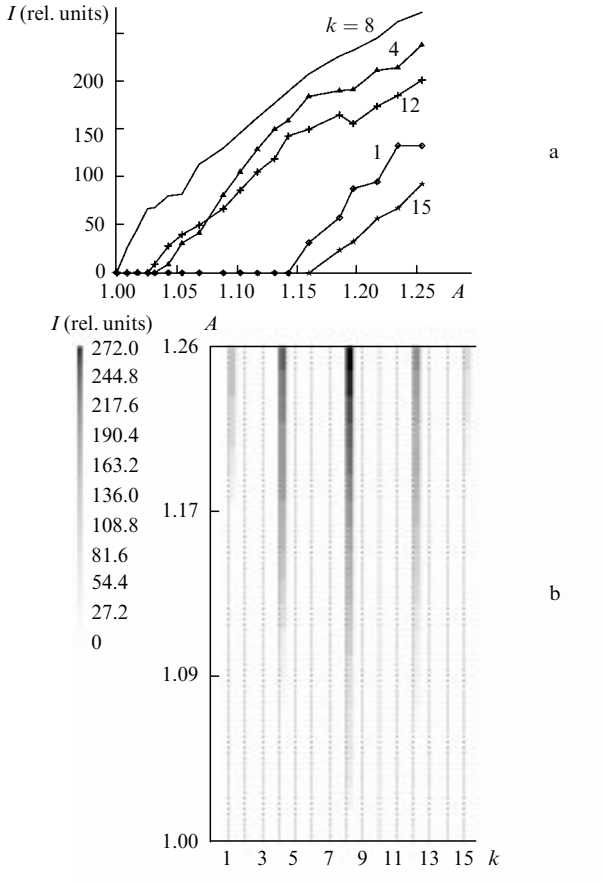


**Figure 3.** Dependences of the optical-mode intensities on the pump parameter $A$ in the two-dimensional (a) and three-dimensional (b) representations for $L_{opt} = 8.3$ cm.

neighbouring longitudinal indices were virtually absent in the experiments and the spectrum was to a large degree symmetric and stable.

A similar series of experiments was carried out with a shorter cavity of length $L_{opt} = 5.7$ cm [$\Delta\nu = c \times (2L_{opt})^{-1} = 2.6$ GHz]. In this case, the optical spectrum of an Nd : YAG laser was studied with the aid of a Fabry – Perot etalon having a 2.4 mm base, which corresponded to free spectral range of $\sim$63 GHz. The width of the etalon mode was close to 0.5 GHz. The dynamics of variation of the optical spectrum of a strong-polarisation mode with changes in the pump parameter was studied (Fig. 4a). The number of modes participating in lasing varied from one to five under these conditions. As can be seen from the photographs, the optical spectrum was not equidistant. The side modes began to lase asymmetrically: on increase in the pumping rate, the centre of the optical spectrum shifted to the low-frequency region (to the left). Measurements showed that the spacing between the lasing modes was $4.8 \pm 0.6$ and $7.8 \pm 0.9$ GHz, which corresponded to two ($2.6 \times 2 = 5.2$ GHz) and three ($2.6 \times 3 = 7.8$ GHz) elementary mode spacings $\Delta\nu$. This means that one or two longitudinal modes, located between two lasing modes, were suppressed.

A three-dimensional plot of the dependences of the lasing-mode intensities on the pump parameter is given in Fig. 5. It takes into account their positions on the frequency axis. The longitudinal modes behave similarly in the case of weak polarisation (Fig. 4b). The threshold pump parameter for a weak-polarisation mode is $A = 1.3$. The number of the longitudinal modes with weak polarisation is smaller than in the case of strong polarisation, but the frequency differences between the lasing modes are the same in both cases. It is noteworthy that, in contrast to the case of a long cavity, in this cavity configuration the optical spectrum exhibited a significant instability for both polarisations. This was manifested by frequent jumps from one longitudinal mode to neighbouring modes, which can be clearly seen in Fig. 5. The cause of such behaviour could have been the higher sensitivity, under these conditions, of the laser to the changes in the optical length of the cavity, which were not monitored in the experiment.

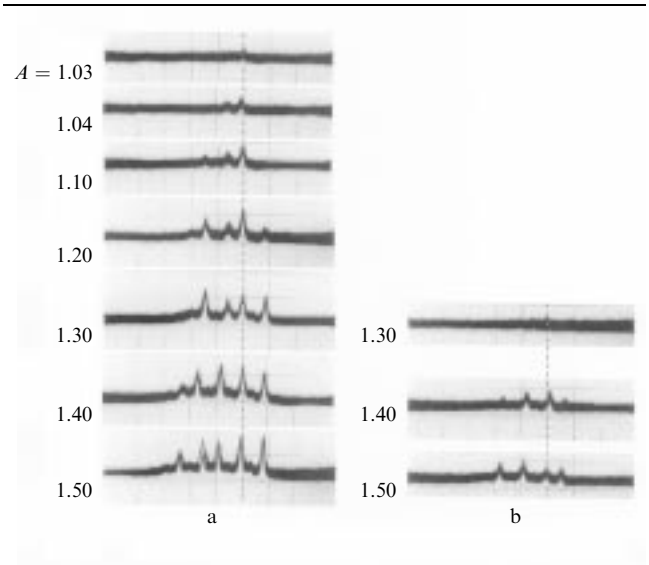


**Figure 4.** Dynamics of the optical spectrum with increase in the pump parameter $A$ for strong (a) and weak (b) polarisation modes.

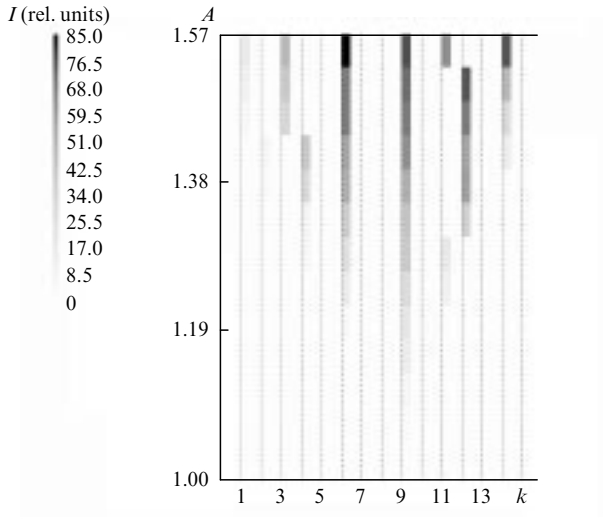


**Figure 5.** Dependences of the optical-mode pump intensities on the pump parameter $A$ in the three-dimensional representation for $L_{opt} = 5.7$ cm.

The experimental study of the optical spectrum of a linear Nd : YAG laser with the active element placed flush against the input mirror of the cavity yielded the following results for small cavity fill factors (0.2 and 0.3). The emission spectrum is significantly 'rarefied'. The frequency differences between the lasing modes vary from two to four mode spacings of a cold cavity. A reduction in the fill factor leads to a greater 'rarefaction' of the spectrum and then the lasing modes become more immune to external perturbations and to the competitive influence of the neighbouring longitudinal modes.

## 4. Comparison of experimental and theoretical results

In order to compare the theory with experiment, we integrated numerically the system of equations (5), formulated for the case involving possible lasing of 20 modes. If the gain-line profile is Lorentzian, the gain $g_k$ can be described by:

$$g_k = \left\{1 + \left[\left(\frac{K}{2} + 1 - k\right)\delta - \delta_0\right]^2\right\}^{-1}.$$

Here, $k = 1, 2, \ldots, K$; $K = 20$; $\delta$ and $\delta_0$ are, respectively, the mode spacing and the detuning relative to the centre of the mode-gain line ($k = 11$) closest to the latter, both normalised to the half-width of the gain line. If the gain line width is $\sim$160 GHz (in Refs [12] and [13], it was 135 and 195 GHz, respectively), we obtain $\delta = 0.021$ ($L_{opt} = 8.3$ cm) and $\delta = 0.03$ ($L_{opt} = 5.7$ cm) for our experimental conditions. In order to ensure an asymmetric situation when all the modes have different gains, the detuning $\delta_0 \approx \delta/4$ was used in the numerical calculation. Different values of the absorption coefficient $\alpha$ have been quoted in the literature: from 3 to 8 cm$^{-1}$ at the wavelength of 808 nm [14]. According to our measurements, $\alpha = 3 - 4.5$ cm$^{-1}$. One of the causes of the spread of the absorption coefficients may be variation of the laser diode temperature with the laser diode current, causing a shift of the emission frequency.

In our numerical integration of the system of equations (5), the parameter $\alpha l$ was assumed to be 3.5. Fig. 6 presents, as an example, the results of a numerical calculation

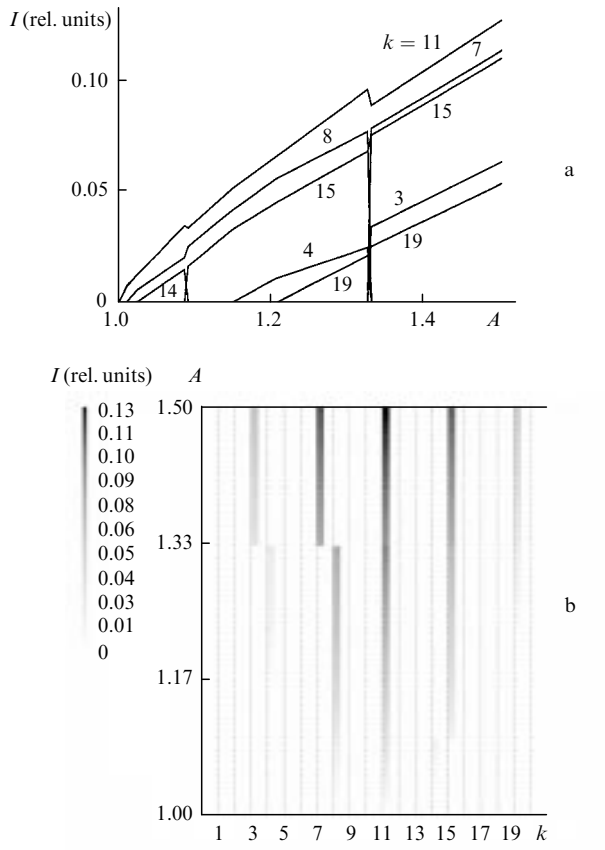


**Figure 6.** Theoretical dependences of the optical-mode intensities on the pump parameter $A$ in the two-dimensional (a) and three-dimensional (b) representations for $G = 2500$, $l/L = 0.22$, $\delta = 0.021$, $\delta_0 = \delta/4$, $\alpha = 3.5\ \mathrm{cm}^{-1}$.

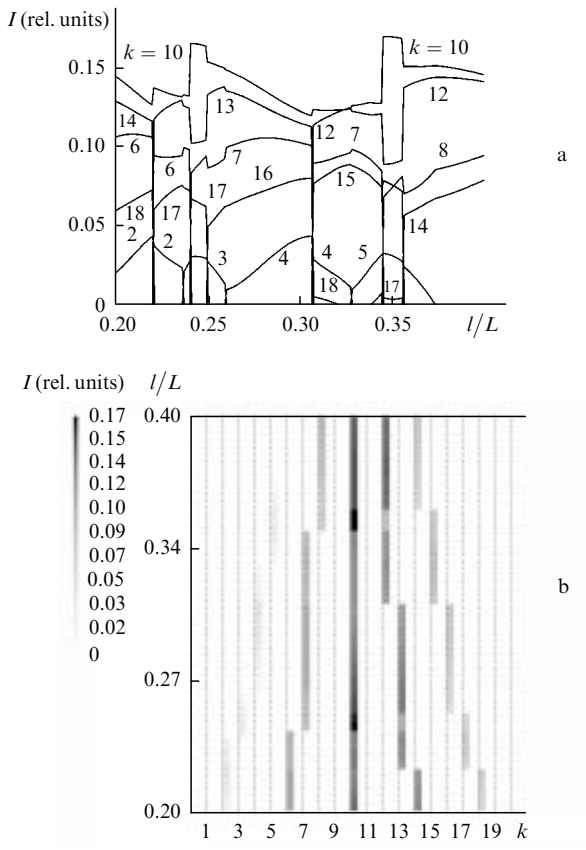


**Figure 7.** Theoretical dependences of the optical-mode intensities on the factor $l/L$ representing filling of the cavity with the active medium in the two-dimensional (a) and three-dimensional (b) representations for $G = 2500$, $A = 1.5$, $\delta = 0.030$, $\delta_0 = \delta/4$, $\alpha = 3.5\ \mathrm{cm}^{-1}$.

of the behaviour of the mode intensity as the pump parameter is varied, carried out for the factor $l/L = 0.22$ representing filling of the cavity with the active medium. Similar calculations were performed also for $l/L = 0.32$. Comparison with experimental data (Figs 3 and 5) shows that the model system of equations (5) describes quite satisfactorily the dynamics of the optical spectrum of a multimode solid-state laser with an nonuniform longitudinal distribution of the gain. First, this applies to the frequency interval between the lasing modes. A decrease in the fill factor increases this frequency interval, in full agreement with the experiment. Furthermore, for the pump-radiation absorption parameter selected in the calculations, an agreement is observed between the calculated number of the suppressed modes and the experimentally observed number. Furthermore, it is seen from Fig. 6 that a change in the pumping rate leads to jumps to neighbouring longitudinal modes. This can also be one of the causes (together with technical fluctuations in the parameters, for example in the length of the cavity) of the mode jumps observed in the experiment.

Fig. 7 illustrates the behaviour of the longitudinal-mode intensities as the cavity fill factor is varied. The real situation as regards variation of the fill factor $l/L$ because of variation of the optical length of the cavity, accompanied by a proportional change in the mode spacing $\delta$, was modelled in the calculation. It is seen from Fig. 7 that, with decrease in $l/L$, new longitudinal cavity modes become involved in the lasing. On the other hand, the number of the lasing modes hardly changes, whereas the interval between them increases from two to four mode spacings. The width of the emission spectrum changes very slightly under these conditions. This is related to a twofold reduction in the fill factor accompanied by the same reduction in the mode spacing.

It follows from Fig. 7, that for $l/L \sim 0.2$ all 20 modes are involved in the lasing. Evidently, a further reduction in $l/L$ should lead to an even greater increase in the number of the longitudinal modes participating in the lasing. However, restriction of the system of equations (5) to twenty modes, which we adopted, precluded demonstration of this effect and there is therefore no point in analysing a fill factor smaller than 0.2.

The nature of the influence of the exponential absorption of the pump radiation can be seen from Figs 8 and 9, demonstrating the dynamics of the optical spectrum as the absorption coefficient $\alpha$ is varied for $l/L = 0.22$ and 0.32 achieved in our experiment. It is seen from Figs 8 and 9 that the exponential attenuation ($0 < \alpha < 0.1$) leads to a marked 'rarefaction' of the spectrum. A further increase in $\alpha$ is accompanied by abrupt hopping between certain neighbouring modes, which is accompanied by abrupt changes in the lasing-mode intensities.

It must be emphasised that, in the absence of an exponential pumping nonuniformity ($\alpha = 0$), a change in the fill factor occurs without abrupt jumps, although it is accompanied by nonmonotonic changes in the mode intensities. The same applies to complete filling of the cavity ($l/L = 1$): a change in the parameter $\alpha$ is not accompanied by abrupt changes in the mode intensities. The jumps in the mode intensities,

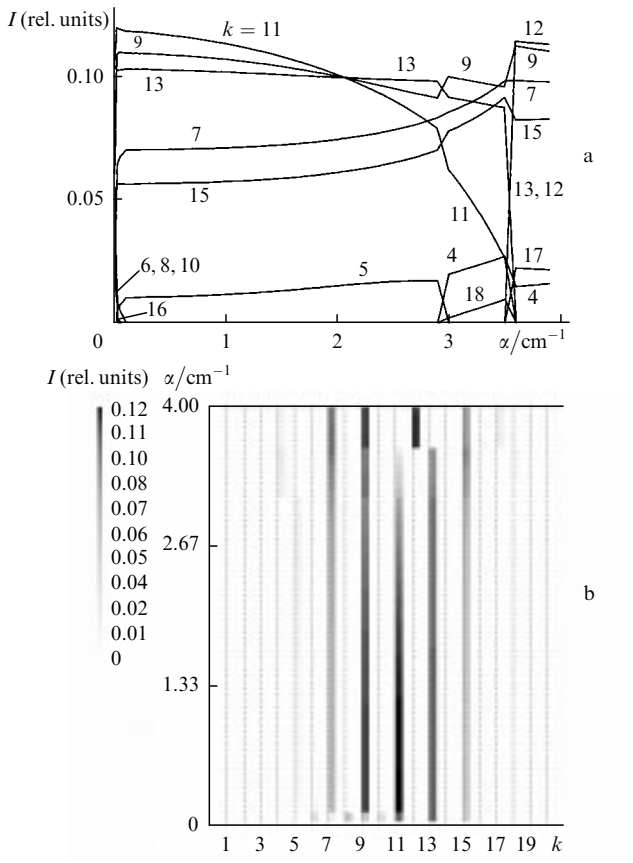


**Figure 8.** Theoretical dependences of the optical-mode intensities on the pump-radiation attenuation coefficient $\alpha$ in the two-dimensional (a) and three-dimensional (b) representations for $G = 2500$, $A = 1.5$, $l/L = 0.22$, $\delta = 0.021$, $\delta_0 = \delta/4$.

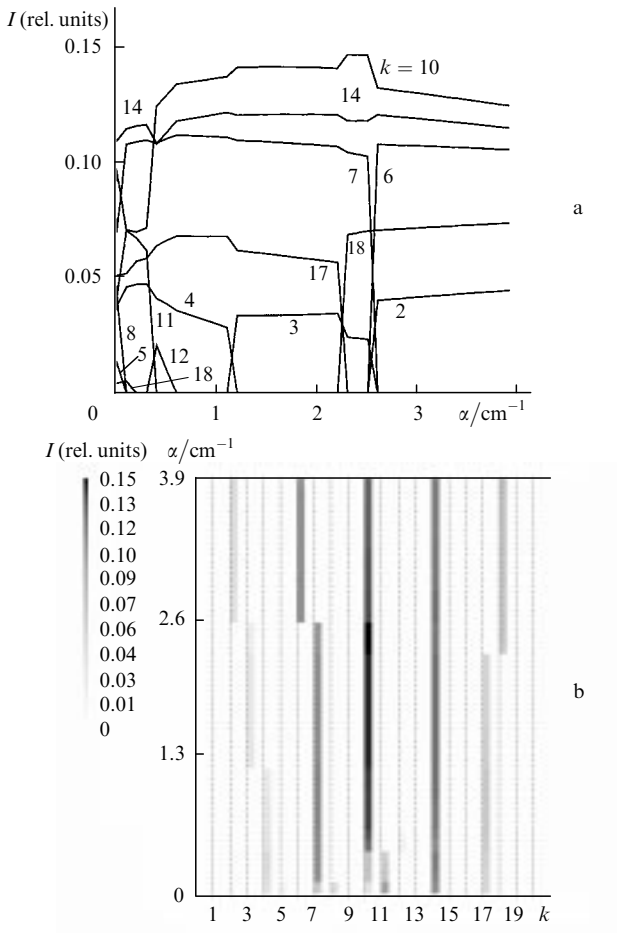


**Figure 9.** The same dependences as in Fig. 8, but for $l/L = 0.32$ and $\delta = 0.030$.

including hopping to the neighbouring modes, are characteristic only of the joint operation of the two mechanisms of the longitudinal gain nonuniformity along the cavity, considered above. It can be seen from Figs 8b and 9b that, in order to obtain a qualitative agreement between the theory and experiment, the parameter $\alpha$ must be in the range $2 < \alpha < 4$. This virtually agrees with the direct measurements of $\alpha$ carried out in the present study.

## 5. Discussion of results and conclusions

Our experimental study of the optical spectrum of a solid-sate laser demonstrated that a reduction from 0.32 to 0.22 in the factor representing filling of the cavity by the active medium leads to 'rarefaction' of the optical spectrum: the number of modes excited between neighbouring lasing modes increases from one – two to two – three, respectively. The characteristics of the optical radiation spectrum observed in our experiment can be accounted for within the framework of the theory developed above.

This communication proposes a model of a solid-state laser with a Fabry – Perot cavity, in which account is taken of an nonuniform distribution of the unsaturated gain along the laser axis caused both by absorption of the pump radiation along the crystal and by partial filling of the laser cavity with the active medium. The proposed model remains within the framework of the approximation generally adopted for a homogeneous pump intensity distribution. In this approximation, no account is taken of the influence on the laser dynamics of large-scale population-inversion $D_p^s(\tau)$ gratings arising from the saturating effect exerted by the lasing modes. The large-scale inversion gratings due to the longitudinal pump nonuniformity (the unsaturated part of the population inversion) are then taken into account in the model by introducing additional terms in the equations for the mode intensities, compared with the simplest case of a homogeneous pump intensity distribution along the length of the cavity. In this approach, the dimensionality of the model represented by the system of equations (5) remains the same as for a homogeneous longitudinal distribution of the unsaturated gain $(2K + 1)$.

A calculation based on the model proposed by Pieroux and Mandel [10] showed that the behaviour of the intensities agrees with a calculation based on the model described by the system of equations (5), whereas the steady-state grating amplitudes $\bar{D}_p^s = \bar{D}_p - \bar{D}_0\Phi_p$ remain virtually in the range $0.01\bar{D}_0 - 0.03\bar{D}_0$ as regards order of magnitude, both in the absence of an nonuniform gain distribution ($l/L = 1$ and $\alpha = 0$) and throughout the range of variation of the parameter $l/L$ and $\alpha$ in which the 20-mode generation approximation remains valid. These calculations justify the chosen approximation for calculation of steady states and for study of the low-frequency dynamics of solid-state lasers.

The generation of orthogonally polarised modes has actually been observed experimentally. Studies have shown that the polarisation interaction between modes does not

influence the 'rarefaction' of the optical spectrum in the multimode emission by a solid-state laser. The validity of this conclusion may be inferred from Fig. 4a, where the photographs 1 – 4 were obtained at low pump intensities when the orthogonally polarised modes have not as yet become involved in the lasing. Under these conditions, the polarisation interaction of the modes does not affect 'rarefaction' of the optical spectrum. It is manifested only in the low-frequency dynamics as additional relaxation oscillations [11].

It is noteworthy that linearly polarised pump radiation leads to a polarisation nonuniformity of the gain [11], influencing the character of the polarisation mode interaction. Evidently, it is more convenient to use a model with an initially lower dimensionality as the starting point for the description of the characteristics of multimode emission by a bipolarisation solid-state laser, because the inclusion (in the system) of orthogonal modes and angular population-inversion harmonics leads to an appreciable increase in the dimensionality of the system (for example, by a factor of four [12]).

A model described by the system of equations (5) which we developed also makes possible an analytical search for steady states: a procedure designed to search for steady states has been proposed for the case when account is taken only of the exponential decrease in the pump intensity along the crystal [4]. There are no fundamental difficulties in extending it to the case of an arbitrary longitudinal gain nonuniformity.

**Acknowledgements.** The authors take this opportunity to express their gratitude to Ya I Khanin for a fruitful discussion of the results and the critical comments in the course of this study. The study was supported by the Russian Foundation for Basic Research (Grants Nos 96-02-19274 and 96-15-96742).

## References

1. Kovalenko E S *Izv. Vyssh. Uchebn. Zaved. Radiofiz.* **10** 1765 (1967);
   Kovalenko E S, Shangina L I *Izv. Vyssh. Uchebn. Zaved. Radiofiz.* **12** 846 (1969);
   Gusev A A, Kruzhalov S V, Pakhomov L N, Petrun'kin V Yu *Pis'ma Zh. Tekh. Fiz.* **4** 1250 (1978) [*Sov. Tech. Phys. Lett.* **4** 503 (1978)];
   Mironenko V R, Yudson V I *Opt. Commun.* **41** 126 (1982);
   Evtyukhov K N, Kaptsov L N, Mitin I V *Zh. Prikl. Spektrosk.* **32** 18 (1980);
   Viktorov E A, Sokolov V A, Tkachenko E V, Ustyugov V I *Opt. Spektrosk.* **68** 920 (1990) [*Opt. Spectrosc. (USSR)* **68** 537 (1990)]
2. Evdokimova O N, Kaptsov L N *Kvantovaya Elektron. (Moscow)* **16** 1557 (1989) [*Sov. J. Quantum Electron.* **19** 1001 (1989)]
3. Abraham N B, Sekaric L, Carson L L, Seccareccia V, Khankokhin P A, Khanin Ya I, Koryukin I V, Zhislina V G (in press)
4. Stamatescu L, Hamilton M W (in press)
5. Tang C L, Statz H, deMars G *J. Appl. Phys.* **34** 2289 (1963)
6. Khanin Ya I *Principles of Laser Dynamics* (North-Holland: Amsterdam, 1995)
7. Mandel P *Theoretical Problems in Cavity Nonlinear Optics* (Cambridge: Cambridge University Press, 1997)
8. Khandokhin P A, Mandel P, Koryukin I V, Nguen B A, Khanin Ya I *Phys. Lett.* **235** 248 (1997)
9. Khandokhin P A, Khanin Ya I, Celet J-C, Dangoisse D, Glorieux P *Opt. Commun.* **123** 372 (1996)
10. Pieroux D, Mandel P *Quantum Semiclass. Opt.* **9** L17 (1997)
11. Khandokhin P A, Ovchinnikov E A, Shirokov E Yu *Phys. Rev. A* (in press)
12. Khandokhin P A, Khanin Ya I, Mamaev Yu, Milovskiĭ N, Shirokov E, Bielawski S, Derozier D, Glorieux P *Kvantovaya Elektron. (Moscow)* **25** 517 (1998) [*Quantum Electron.* **28** 502 (1998)];
    Khandokhin P, Khanin Ya, Mamaev Yu, Milovsky N, Shirokov E, Bielawski S, Derozier D, Glorieux P *Quantum Semiclass. Opt.* **10** 97 (1998);
    Khandokhin P A, Milovsky N D, Mamaev Yu A, Ovchinnikov E A, Shirokov E Yu *Proc. SPIE Int. Soc. Opt. Eng.* **3682** 53 (1998)
13. Koechner W *Solid-State Laser Engineering* (Berlin: Springer, 1993)
14. Zverev G M, Golyaev Yu D *Lazery na Kristallakh i Ikh Primenenie* (Crystal Lasers and Their Applications) (Moscow: Radio i Svyaz', 1994)
15. Fan T Y, Byer L *IEEE J. Quantum Electron.* **23** 605 (1987)